

STM measurement of single spin relaxation time in superconductors.

Jurij Šmakov^{1,2}, Ivar Martin², and Alexander V. Balatsky²

¹*Theoretical Physics, Department of Physics, Royal Institute of Technology, SE-10044 Stockholm, Sweden*

²*Theoretical Division, Los Alamos National Laboratory, Los Alamos, NM 87545*

(Printed November 4, 2018)

Localized spin states in conventional superconductors at low temperatures are expected to have long decoherence time due to the strong suppression of spin relaxation channels. We propose a scanning tunneling microscopy (STM) experiment allowing the direct measurement of the decoherence time of a single spin in a conventional superconductor. The experimental setup can be readily applied to general-purpose spin-polarized STM and to local spin relaxation spectroscopy. A possible extension of the setup to a quantum information processing scheme is discussed.

When a magnetic atom is placed in a conventional s -wave superconductor, the exchange interaction between the localized spin and the conduction electrons leads to formation of *spin polarized* scattering resonances inside the superconducting energy gap [1–3]. These resonances manifest themselves as sharp peaks in the density of states localized near the impurity. The spin-relaxation time for such states is governed by the coupling to the environment. At low temperatures, this coupling is strongly suppressed due to the gapped nature of quasiparticles in s -wave superconductors. The weak spin-relaxation channels related to magnetic dipole-dipole interaction with the nuclear magnetic moments can be further reduced by choosing a superconductor with zero nuclear spin. It is therefore expected that long spin-relaxation times are achievable when a local moment is placed in s -wave superconductor. In this Letter we propose an experimental setup capable of determining the single-spin relaxation time for such defects. Provided that the measured spin-relaxation time is sufficiently long, superconducting tips ending with a single magnetic atom can be used for low-temperature spin-polarized STM. We also discuss a possible application of the spin-polarized local states in superconductors in quantum information processing schemes.

The tunneling current between two spin-polarized states depends strongly on the angle between the respective spin polarizations. The time-dependence of the tunneling current can hence be used to extract the dynamics of the individual spins, assuming they are weakly coupled. This is the basis for our method of determination of the single-spin relaxation time in superconductors. In the proposed experiment, both sides of the tunnel junction are identical superconductors, each containing one magnetic atom. The spin-polarized signal will be optimized when the impurities on the two sides of the junction are spatially aligned; this is most easily achieved in the STM setup, when one of the magnetic atoms is placed directly on the tip. Superconducting (for example, Nb) STM tips have already been successfully used [4] and the STM capabilities for the single-atom manipulation [5] make the fabrication of the tip ending with a single magnetic impurity atom feasible.

To theoretically predict the dependence of the I - V characteristic on the angle between the impurity spins on the tip and on the surface, we use the T -matrix approach, combined with the tunneling Hamiltonian formalism. We model the impurity by introducing a local perturbation to the Bardeen-Cooper-Schrieffer (BCS) Hamiltonian describing a homogeneous superconductor. In the Nambu formalism [6], the impurity Hamiltonian can be written in terms of two-component Nambu spinors, $\Psi_{\mathbf{k}} = [c_{\mathbf{k}\uparrow} \ c_{-\mathbf{k}\downarrow}^\dagger]^T$, as [2]

$$H_{\text{imp}} = \frac{1}{N} \sum_{\mathbf{k}\mathbf{k}'} \Psi_{\mathbf{k}}^\dagger \hat{V} \Psi_{\mathbf{k}'}. \quad (1)$$

Here $\hat{V} = W\hat{\tau}_0 + U\hat{\tau}_3$, $\hat{\tau}_0$ is the 2×2 unit matrix, $\hat{\tau}_i$ ($i = 1, 2, 3$) are the Pauli matrices. The impurity strength is characterized by the exchange interaction with the conduction electrons, W , and the on-site potential, U , or the corresponding dimensionless parameters $w = \pi N_0 W$ and $u = \pi N_0 U$, where N_0 is the density of states at Fermi level in the normal state. We can then obtain the expression for the complete finite-temperature Green's function (GF) in the presence of single impurity,

$$\hat{G}(\mathbf{r}, \mathbf{r}'; i\omega) = \hat{G}^{(0)}(\mathbf{r} - \mathbf{r}'; i\omega) + \hat{G}^{(0)}(\mathbf{r}; i\omega) \hat{T}(i\omega) \hat{G}^{(0)}(-\mathbf{r}'; i\omega), \quad (2)$$

in terms of the GF for the homogeneous SC $\hat{G}^{(0)}(\mathbf{r}; i\omega)$ and the T -matrix $\hat{T}(i\omega) = [\hat{V}^{-1} - \hat{G}^{(0)}(\mathbf{r} = 0; i\omega)]^{-1}$. We approximate the finite-temperature GFs for the homogeneous SC in the real-space representation by

$$\hat{G}^{(0)}(\mathbf{r}; i\omega) = -\frac{\pi N_0 [i\omega \hat{\tau}_0 + \Delta \hat{\tau}_1] \sin k_F r}{\sqrt{\omega^2 + \Delta^2} k_F r}, \quad (3)$$

where 2Δ is the SC energy gap and k_F is the Fermi momentum. By using expression (3) we neglect the exponential decay of the GF for the homogeneous superconductor with $r = |\mathbf{r}|$ on the length scale of the superconducting coherence length (typically ~ 1000 Å for conventional SCs) and the effects of the finite bandwidth. Both approximations are justified, because we are only interested in short-length (of the order of few Ångströms) and low-frequency (of the order of SC gap) behavior of the GF. We also neglect the suppression

of the SC order parameter in the vicinity of the impurity, because this approximation does not significantly affect the spectral functions [2]. Using this set of approximations, we calculate the GF for a superconductor with an impurity and found the expressions for the spectral functions, corresponding to its diagonal elements $A_{ii}(\mathbf{r}, \mathbf{r}'; \epsilon) = -(1/\pi)\text{Im} G_{ii}^R(\mathbf{r}, \mathbf{r}'; \pm\epsilon)$. Here the plus sign in the argument of the retarded GF $G_{ii}^R(\mathbf{r}, \mathbf{r}'; \epsilon)$, obtained by analytic continuation of (2), corresponds to $i = 1$ and minus sign to $i = 2$. Spectral functions A_{ii} have a particle-hole-symmetric continuous part at frequencies $|\epsilon| > \Delta$ and a δ -function singularities on the symmetric energies,

$$\epsilon_0 = (-)^i \frac{\alpha\Delta}{\sqrt{1+\alpha^2}}, \quad (4)$$

where $\alpha = (1 + u^2 - w^2)/(2w)$.

In the tunneling Hamiltonian formalism, the quasiparticle tunneling current can be expressed as a convolution of the spectral functions on different sides of the junction [7]. In our case, the impurities on the tip and on the surface (we will use sub- or superscript “1” to refer to the tip properties and “2” for the surface properties) may have different spin orientations. To account for this, we introduce angle θ between the spin directions and express the fermion creation and annihilation operators on the surface in the spin basis with the quantization axis along the tip impurity spin. The result is

$$\begin{aligned} c_{\mathbf{r}_2\uparrow}^\dagger &= \cos\frac{\theta}{2}c_{\mathbf{r}_2\uparrow}^\dagger + \sin\frac{\theta}{2}c_{\mathbf{r}_2\downarrow}^\dagger, \\ c_{\mathbf{r}_2\downarrow}^\dagger &= -\sin\frac{\theta}{2}c_{\mathbf{r}_2\uparrow}^\dagger + \cos\frac{\theta}{2}c_{\mathbf{r}_2\downarrow}^\dagger. \end{aligned} \quad (5)$$

Here \uparrow , for example, stands for the “up” spin orientation in the surface spin basis and \uparrow is the “up” spin in the tip spin basis. Then, we come to the expression for the total quasiparticle current

$$I(V) = (I_{11} + I_{22})\cos^2\frac{\theta}{2} + (I_{12} + I_{21})\sin^2\frac{\theta}{2}, \quad (6)$$

with the partial currents, $I_{ij}(V)$, given by

$$\begin{aligned} I_{ij}(V) &= 2\pi e \sum T_{\mathbf{r}_1, \mathbf{r}_2} T_{\mathbf{r}'_1, \mathbf{r}'_2}^* \int_{-\infty}^{+\infty} \Theta(\epsilon, eV) \times \\ &\times A_{ii}^{(1)}(\mathbf{r}_1, \mathbf{r}'_1; \epsilon) A_{jj}^{(2)}(\mathbf{r}_2, \mathbf{r}'_2; \epsilon - eV) d\epsilon. \end{aligned} \quad (7)$$

Here e is the electron charge, $\Theta(\epsilon, eV) = n_F(\epsilon - eV) - n_F(\epsilon)$ is the difference of the Fermi-Dirac distribution functions on the different sides of the junction, $T_{\mathbf{r}_1, \mathbf{r}_2}$ is the tunneling matrix element, and the summation is performed over all lattice sites on the tip ($\mathbf{r}_1, \mathbf{r}'_1$) and on the surface ($\mathbf{r}_2, \mathbf{r}'_2$). Expression (7) is for general electrode geometry. We can further simplify it by assuming that the tunneling happens from a single point on the tip (the impurity atom). The tunneling matrix element then takes the form $T(r) = T \exp(-\sqrt{r^2 + z^2}/d)$ that depends on the lateral distance r from the projection of the

tip onto the surface, tip-surface distance z , and the characteristic decay length d , related to the material work function (typically about 0.5\AA). Detailed calculations for this and other geometries will be presented elsewhere.

To calibrate the theoretical parameters for the impurity and the superconducting host, we consider tunneling experiment from a *normal* STM tip into the surface of the SC (Nb) with the magnetic adatoms (Gd or Mn) on it [3]. We can qualitatively reproduce experimental tunneling spectra by tuning the impurity parameters w and u . Results of this calculation are presented in Fig. 1. In what follows, we adopt parameters characteristic of Mn adatom in Nb: $w = 0.9$, $u = 1.0$, and $\Delta = 1.48$ meV.

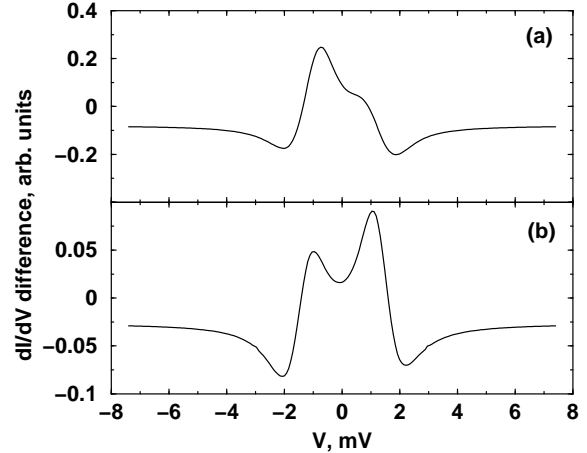


FIG. 1. The calculated change in the dI/dV spectrum due to the presence of Mn (a) and Gd (b) adatoms. Impurity parameters were taken to be $w = 0.9$, $u = 1.0$ for Mn and $w = 0.3$, $u = -0.3$ for Gd. The surface is Nb with $\Delta = 1.48$ meV at $T = 3.85$ K. Tip-surface distance is $z = 5$ \AA and $d = 0.5$ \AA .

When the impurities are present both on the SC tip and on the SC surface, a number of new features appear in the I - V characteristic. For example, when voltage first becomes large enough (in absolute value) for the intragap state of the tip to overlap with the continuous part of the spectrum of the surface, the abrupt increase (or decrease) in current results. The most remarkable feature of these I - V characteristics, however, is their strong dependence on the relative orientation of the impurity spins, i.e. on the angle θ . The reason for this strong dependence is the existence of the contribution to the current, resulting from the overlap between the intragap states of the tip and of the surface (at certain values of voltage). From the expression for the position of the intragap states, Eq. (4), it can be seen that these peaks (generally there are four of them) appear at voltages

$$eV = \pm \frac{\alpha_1 \Delta_1}{\sqrt{1 + \alpha_1^2}} \pm \frac{\alpha_2 \Delta_2}{\sqrt{1 + \alpha_2^2}}. \quad (8)$$

For the identical impurities in the identical superconductors, ($\alpha_1 = \alpha_2$), $\Delta_1 = \Delta_2$, at $\theta = 0$ these peaks vanish because the corresponding intragap states, contributing

to I_{11} and I_{22} overlap only at zero voltage and hence there is no tunneling current between them. Fig. 2 presents the I - V characteristics calculated for various values of angle θ . The δ -function peaks due to the tunneling between the intragap states appear for non-zero θ at $V = \pm 1.63$ mV and become more intensive with increasing θ . It is this strong θ dependence that allows us to formulate the experimental procedure for the measurement of the decoherence time of the intragap impurity spin-polarized states in the SC.

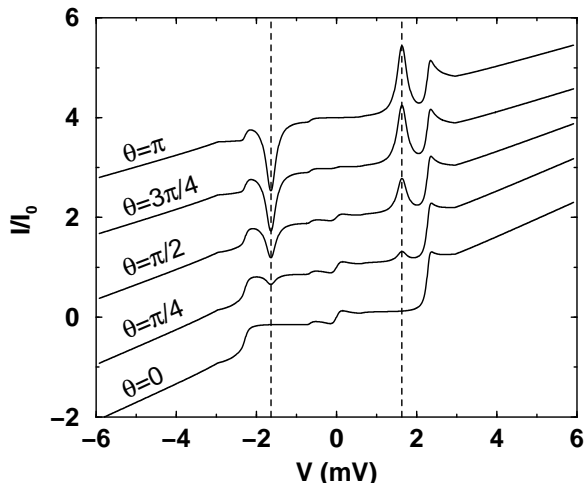


FIG. 2. Calculated I - V characteristic of the Nb superconducting tunneling contact for different values of angle θ between Mn spins on two sides of the junction. The current is normalized by $I_0 = \sigma_0 \Delta_1 / e$, where σ_0 is the normal-state conductance of the tunneling junction. The curves are offset by I_0 and the δ -functions at $V = \pm 1.63$ mV (dashed vertical lines) are broadened for clarity.

The simplest way to measure the spin decoherence time is to monitor time dependence of the tunneling current, $I(t)$, for applied voltage fixed at the resonant value ($V = \pm 1.63$ mV in our calculation). The current-current correlation function, $S(t) = (\langle I(t)I(0) \rangle - \langle I \rangle^2) / (\langle I^2 \rangle - \langle I \rangle^2)$, can be used to directly extract the spin-relaxation time. The theoretical prediction for $S(t)$ is presented in Fig. 3. Another way to extract spin dynamics is to first polarize the spins by external magnetic field (larger than $k_B T / \mu_B$ but smaller than H_{c1}) and then observe the relaxation of the current after the field is removed. The effect of the magnetic dipole-dipole interaction between the impurity spins can be studied by measuring the current relaxation at different tip-surface distances. It is possible, however, that the time resolution of the experiment is insufficient to resolve the times associated with the spin dynamics; in this case, the measured current will be a constant equal to the average value in Eq. (6).

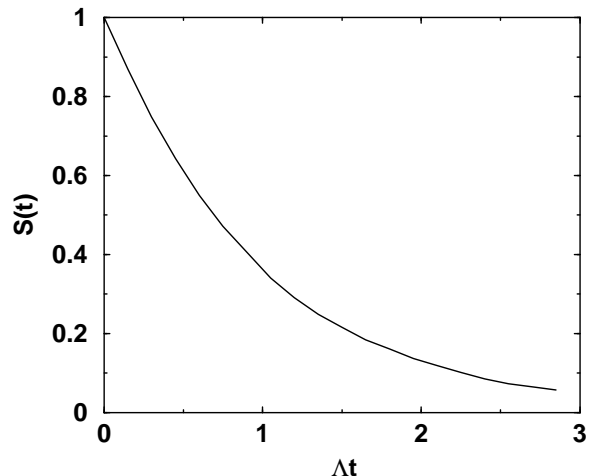


FIG. 3. Current-current correlation function $S(t) = (\langle I(t)I(0) \rangle - \langle I \rangle^2) / (\langle I^2 \rangle - \langle I \rangle^2)$, calculated for uncorrelated diffusion of spin orientations. Assuming that each spin diffuses over the unit sphere with the diffusion coefficient Λ , the relative angle between the spins evolves according to stochastic PDE, $d\theta = \Lambda \cot(\theta) dt / 2 + \sqrt{\Lambda} d\xi$, where ξ is the normal random variable with zero mean and variance $\langle d\xi^2 \rangle = dt$. This correlation function is well approximated by the usual expression for diffusion, $\exp(-\Lambda t)$.

Generally, the same technique may be used to measure the relaxation time of *any* local spin state on a conducting substrate, as long as this relaxation time is shorter than the relaxation time of the impurity-induced intragap state in the SC tip, e.g. Kondo spin dynamics on a metallic surface [8].

If the relaxation time of the intragap spin-polarized impurity state in a SC proves to be sufficiently long, a SC tip ending with a magnetic impurity can be used to obtain the spin-contrast STM images. Currently, to achieve the spin contrast in the STM measurements one has to use ferromagnetic tips [9,10]. These STM experiments have already produced a number of interesting results, like the direct imaging of the two-dimensional antiferromagnetism [9]. Unfortunately, in such setup, the increase of the tunneling area of the tip due to the restrictions on the tip material leads to the degradation of the spatial resolution, compared to conventional STM. In addition, strong magnetic fields produced by the tips may affect the measurements by inducing polarization of the local spin structure, or in the case of superconducting samples, cause a local SC-to-normal transition. Our proposed setup would be the next step in the spin-polarized STM, which would allow the spin-contrast imaging at low biases with an atomically sharp STM tip. In this setup, the effect of the magnetic field due to the magnetization of the tip is minimized since a single impurity spin would be sufficient to achieve the spin contrast. As an example, in Fig. 4, we present a theoretically calculated map of the spin-contrast signal,

$$P = \frac{I_{\uparrow\uparrow} - I_{\uparrow\downarrow}}{I_{\uparrow\uparrow} + I_{\uparrow\downarrow}}, \quad (9)$$

in the vicinity of surface impurity. Currents in Eq. (9) correspond to the parallel ($I_{\uparrow\uparrow}$) and antiparallel ($I_{\uparrow\downarrow}$) orientations of the impurity spins on the tip and on the surface.

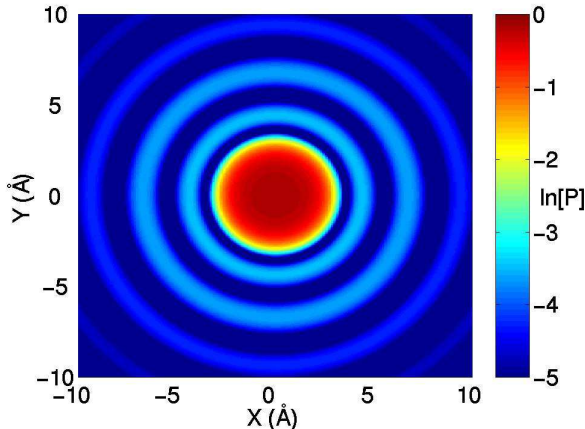


FIG. 4. The topographic map of the log of the spin-contrast STM signal P in the vicinity of the magnetic impurity. Rapidly decaying Friedel oscillations are clearly seen at large distances. For this calculation we have taken the same values of parameters as for Fig. 2 and fixed the bias voltage at $V = 1.63$ mV.

Another application of the spin polarized states near magnetic atoms in superconductors is related to quantum information processing. It is motivated by the expected long relaxation times of spins in s -wave superconductors and the ease of read-out of the spin states using the spin-polarized tunneling techniques discussed above. At temperatures much lower than the SC transition temperature, the quasiparticle contribution to the spin relaxation will effectively disappear. The dipolar relaxation due to interaction with the lattice nuclear spins can be also significantly reduced by using SC with non-magnetic nuclei, e.g. non-magnetic isotopes of Pb or Sn. A local spin in the s -wave superconductor is isolated from environment to the same extent as a local spin in a semiconductor with the band gap equal to 2Δ . An advantage compared to current proposals based of semiconductors, e.g. phosphorus in silicon [11], is that the substrate is

conductive and hence one can do local tunneling experiments to interrogate local spins that store and process quantum information. The details of the proposed quantum information procession architecture based on the local spins in superconductors will be discussed elsewhere [12].

In summary, we have proposed an STM experiment, which will allow the measurement of the decoherence times of the single spins in superconductors. For sufficiently long measured spin-decoherence time, the setup can be applied to the spin-resolved STM measurements. Also, the possibly long decoherence time of the single-impurity spin states in superconductors, combined with the ease of readout and manipulation, make such states a favorable candidate for a qubit in quantum computing applications.

We thank Don Eigler and Gerard Milburn for stimulating discussions. J. Š. would like to thank the Los Alamos National Laboratory for hospitality and gratefully acknowledge partial financial support from the Swedish Research Council.

-
- [1] H. Shiba, Prog. Theor. Phys. **40**, 435 (1968).
 - [2] M. I. Salkola, A. V. Balatsky, and J. R. Schrieffer, Phys. Rev. B **55**, 12648 (1997).
 - [3] A. Yazdani *et al.*, Science **275**, 1767 (1997).
 - [4] S. H. Pan, E.W. Hudson and J. C. Davis, Appl. Phys. Lett. **73**, 2992 (1998).
 - [5] S. Gauthier, Appl. Surf. Sci. **164**, 84 (2000) and references therein.
 - [6] A. L. Fetter, J. D. Walecka, *Quantum Theory of Many-Particle Systems* (McGraw-Hill, San Francisco, 1971).
 - [7] G. D. Mahan, *Many-Particle Physics* (Plenum Press, New York, 1990).
 - [8] H. C. Manoharan, C. P. Lutz, and D. M. Eigler, Nature **403**, 512 (2000).
 - [9] S. Heinze *et al.*, Science **288**, 1805 (2000).
 - [10] W. Wulfhekkel and J. Kirschner, Appl. Phys. Lett. **75**, 1944 (1999).
 - [11] B. E. Kane, Nature **393**, 133 (1998).
 - [12] I. Martin, unpublished.